

Free carrier dynamics of InN nanorods investigated by time-resolved terahertz spectroscopy

H. Ahn, C.-H. Chuang, Y.-P. Ku, and C.-L. Pan

Citation: [Journal of Applied Physics](#) **105**, 023707 (2009); doi: 10.1063/1.3068172

View online: <http://dx.doi.org/10.1063/1.3068172>

View Table of Contents: <http://scitation.aip.org/content/aip/journal/jap/105/2?ver=pdfcov>

Published by the [AIP Publishing](#)

Articles you may be interested in

[Terahertz electroluminescence of surface plasmons from nanostructured InN layers](#)
Appl. Phys. Lett. **96**, 183106 (2010); 10.1063/1.3425897

[Carrier and phonon dynamics of wurtzite InN nanorods](#)
Appl. Phys. Lett. **94**, 071911 (2009); 10.1063/1.3086888

[Time resolved measurements of spin and carrier dynamics in InAs films](#)
J. Appl. Phys. **103**, 064318 (2008); 10.1063/1.2899091

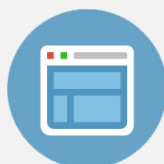
[Time-resolved spectroscopy of recombination and relaxation dynamics in InN](#)
Appl. Phys. Lett. **83**, 4984 (2003); 10.1063/1.1633973

[Carrier relaxation and recombination in GaAs/AlGaAs quantum heterostructures and nanostructures probed with time-resolved cathodoluminescence](#)
J. Appl. Phys. **81**, 3186 (1997); 10.1063/1.364148



Re-register for Table of Content Alerts

Create a profile.



Sign up today!



Free carrier dynamics of InN nanorods investigated by time-resolved terahertz spectroscopy

H. Ahn,^{a)} C.-H. Chuang, Y.-P. Ku, and C.-L. Pan

Department of Photonics and Institute of Electro-optical Engineering, National Chiao Tung University, Hsinchu 30010, Taiwan

(Received 13 August 2008; accepted 3 December 2008; published online 23 January 2009)

Ultrafast time-resolved terahertz spectroscopy is employed to investigate the carrier dynamics of indium nitride (InN) nanorod arrays and an epitaxial film. Transient differential transmission of terahertz wave shows that hot carrier cooling and defect-related nonradiative recombination are the common carrier relaxation processes for InN film and nanorods. However, the electrons confined in the narrow structure of nanorods are significantly affected by the carrier diffusion process near the surface, which causes the abnormally long relaxation time for nanorods. © 2009 American Institute of Physics. [DOI: [10.1063/1.3068172](https://doi.org/10.1063/1.3068172)]

I. INTRODUCTION

Due to its intrinsic narrow bandgap and remarkably large energy difference between the conduction band minimum and the next local minimum, indium nitride (InN) inspires potential applications in the terahertz range. Recently, low-dimensional InN nanomaterials in the forms of nanowires, nanorods, nanotubes, etc., have received great attention due to their importance in near-infrared optoelectronics and photovoltaic applications. Unambiguously, carrier dynamics in these nanomaterials is one of the most important aspects of material properties for optimized performance of optoelectronic applications. Carrier dynamics in semiconductors is typically investigated by using optical pump-probe technique, of which the photon energy of the probe is of the order of the bandgap energy of the samples. The photon energy of terahertz probe is very small (1 THz=4 meV) compared to that of optical probe so that it has a unique capability of examining the ultrafast relaxation mechanisms of free electrons, which can provide the essential information for device design and optimization. Several results on the ultrafast carrier dynamics of InN epilayers have been reported by using time-resolved optical¹⁻⁴ or terahertz spectroscopy,⁵ but no systematic study has been reported on carrier dynamics of InN nanostructures. In the present work, we report on the carrier dynamics of InN nanorods compared to that of InN epilayer measured by optical pump-terahertz probe technique.

Previously, we have reported a significant enhancement of terahertz emission from InN nanorod arrays compared to that from InN epilayer.⁶ The major terahertz emission mechanism of InN film has been proposed to be the photo-Dember effect, which is driven by the transient current due to the difference of diffusion velocities of electrons and holes. Furthermore, a modified photo-Dember effect is suggested to explain the enhancement mechanism of terahertz emission from the nanorods, where terahertz emission depends on the size and aerial density of the nanorods. A tera-

hertz time-domain spectroscopy (TDS) measurement showed that InN nanorods have much shorter Drude scattering time constant than InN film, which may be due to the less perfect crystalline quality of the nanorods as well as the geometrical confinement of mobile carriers in the rods.⁷ Since terahertz emission is based on the transient behavior of the carriers, it is essential to characterize the carrier dynamics of InN films and nanorods in order to understand terahertz emission mechanism from these samples. Time-resolved terahertz transmission measurement allows us to study the transient optical responses and electron transfer mechanism of vertically aligned InN nanorod arrays, which cannot be explained by the static measurement techniques such as terahertz TDS. Distinctively fast decay of photoexcited carrier density is observed for the InN nanorod arrays compared to the InN films, which is attributed to the defect-related electron trapping and the increased interaction with the boundaries of nanorods. Additionally for nanorods, reduced diffusion rate in the vicinity of the surface is found to play an important role in the carrier relaxation dynamics at the long time delay.

II. EXPERIMENT

In these measurements, ultrafast optical pump was provided by a Ti:sapphire regenerative amplifier laser system, which delivers ~50 fs optical pulses at a center wavelength of 800 nm with a repetition rate of 1 kHz. The terahertz probe beam was generated from a photoexcited (100) InAs surface and detected by free-space electro-optic sampling in a 2-mm-thick ZnTe crystal. In the optical pump-terahertz probe experiment, the transient behavior of the photoexcited carriers was monitored by measuring the transmitted peak amplitude of terahertz waveforms at normal incident angle as a function of delay time between the terahertz probe and optical pump pulses. The static electrical properties of the samples were separately measured by a terahertz-TDS system based on low-temperature-grown GaAs photoconductive dipole antennas, which were excited and probed by a Ti:sapphire laser at a repetition rate of 82 MHz. All the measurements were done under dry nitrogen purge.

^{a)}Author to whom correspondence should be addressed. Electronic mail: hyahn@mail.nctu.edu.tw.

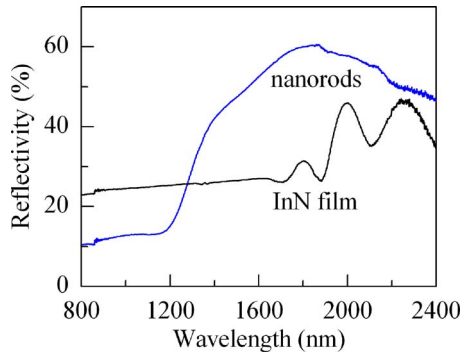


FIG. 1. (Color online) Near-infrared reflectivity of InN film and nanorods measured at normal incidence.

For this work, a wurtzite InN epitaxial film and vertically aligned InN nanorod arrays were grown on Si(111) substrates by plasma-assisted molecular-beam epitaxy. The InN epilayer was grown on Si(111) using the epitaxial AlN/ β -Si₃N₄ double-buffer layer technique.⁸ The InN nanorods were grown at a sample temperature of 330 °C on β -Si₃N₄/Si(111) without the AlN buffer layer. The scanning electron microscopy (SEM) image of the hexagonal-shaped nanorods exhibits nanorods with a uniform diameter of ~ 130 nm and an average aspect ratio (height/diameter) of ~ 6 . The nanorod arrays have an aerial density of $\sim 5 \times 10^9$ cm⁻². The thicknesses of the InN epilayer and nanorods are about 1.0 and 0.75 μ m, respectively. The morphology and size distribution of InN nanorods were analyzed using SEM. Electrical characteristics were measured by terahertz TDS,⁷ and the characteristics are as follows: InN epilayer film has a carrier density $N_e = (2.5 \pm 0.2) \times 10^{18}$ cm⁻³ and a carrier mobility $\mu = 1217 \pm 58$ cm²/V s, while nanorods have $N_e = (4.9 \pm 0.2) \times 10^{19}$ cm⁻³ and $\mu = 80 \pm 5$ cm²/V s. The corresponding plasma frequencies of InN film and nanorods are 52 ± 1.2 and 199 ± 3 THz, respectively. Figure 1 shows near-infrared reflectivity of InN film and nanorods measured at the wavelength covering from 800 to 2400 nm. The oscillation of reflectivity of InN film is due to the light interference within the thin film in the transparent region below the bandgap energy. Meanwhile, the decrease in reflectivity of InN nanorods at the wavelength below 1500 nm (≈ 199 THz) is attributed to the collective behavior of electrons and holes above the plasma frequency. The reflectivity responses at the pump wavelength (800 nm) show that InN nanorods absorb more light than InN film, which is due to the increased surface-to-volume ratio for nanorods.

III. DATA AND DISCUSSION

Figure 2 shows the time-dependent differential transmission signals of InN nanorods (blue) and the epilayer (black): $\Delta T_{\text{terahertz}}/\Delta T_{\text{terahertz}}^0$, where $\Delta T_{\text{terahertz}}^0$ is the transmitted intensity of terahertz probe through the unexcited sample. Each sample is excited at the laser fluence of 1.1 mJ/cm². As soon as the pump pulse arrives, transmission responses of both samples instantaneously drop and the sample-independent sharp fall time is measured to be 0.6–0.7 ps. Due to our relatively broad pulsewidth of terahertz probe

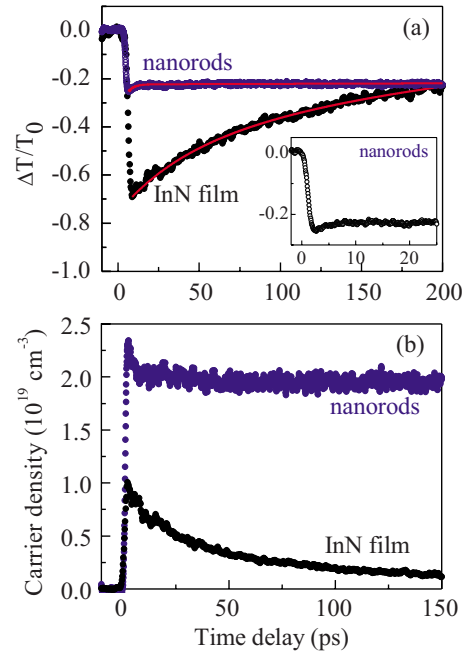


FIG. 2. (Color online) (a) Differential terahertz transmission dynamics, $\Delta T_{\text{terahertz}}/T_{\text{terahertz}}^0$ due to 800 nm excitation for nanorods (blue) and the InN epilayer (black). The excitation fluence is 1.1 mJ/cm². Inset: $\Delta T_{\text{terahertz}}/T_{\text{terahertz}}^0$ of nanorods in the expanded scale. The solid lines are the results of biexponential fitting as described in the text. (b) The photoexcited carrier density of InN film and nanorods calculated by Eq. (2).

(~ 0.6 ps) and the slow detector response time, sample-dependent fall time cannot be monitored. The transmission response of InN film gradually recovers from 70% to $\sim 22\%$ within 200 ps, while that of nanorods quickly recovers to its steady value within 2 ps and persists at this value over 200 ps.

The solid lines in Fig. 2(a) are obtained from a biexponential fit,

$$\Delta T_{\text{terahertz}}/T_{\text{terahertz}}^0 = \Delta T_{\text{terahertz}}^{\text{max}} [-Ae^{-t/\tau_1} + (A-1)e^{-t/\tau_2}], \quad (1)$$

where $\Delta T_{\text{terahertz}}^{\text{max}}$ is the maximum transmission change, A is the weighting factor, and τ_i are relaxation time constants. Single exponential recovery function results in poor fitting for each sample. According to the best fit parameters listed in Table I, the initial fast relaxation time (τ_1) of nanorods is 2.6 ± 0.5 ps and that for InN film is 30.7 ± 0.9 ps. The slow relaxation time (τ_2) of the InN film is 194 ± 2.5 ps, but that of nanorods is much longer (> 7 ns) and its accurate value cannot be determined by our system with a limited scanning range. From the measured $\Delta T_{\text{terahertz}}/T_{\text{terahertz}}^0$ data, the time-dependent carrier density in a photoexcited sample can be calculated by the relation⁹

$$N(t) = \frac{1+n}{Z_0 e \delta \mu} \left[\left(1 + \frac{\Delta T_{\text{terahertz}}}{T_{\text{terahertz}}^0} \right)^{-1} - 1 \right], \quad (2)$$

where $n=3.3$ is the refractive index for silicon substrate in the terahertz range,¹⁰ $\delta=133$ nm is the optical penetration depth of 800 nm light,¹¹ and $Z_0=377 \Omega$ is the impedance of free space. With the electron mobilities measured by terahertz TDS, $N(t)$ is calculated for nanorods and film and

TABLE I. Summary of the biexponential fitting results for InN film and nanorods. The carrier scattering time τ_0 and electron mobilities are obtained from a separate terahertz-TDS measurement (Ref. 7).

Sample	$\Delta T_{\text{terahertz}}^{\text{max}}$	A	τ_1 (ps)	τ_2 (ps)	τ_0^a (fs)	μ^a (cm ² /V s)	ω_p^a (THz)
InN film	0.7	0.29	30.7 ± 0.9	194 ± 2.5	52 ± 2.5	1217 ± 58	52 ± 1.2
Nanorods	0.26	0.12	2.6 ± 0.5	>7000	13 ± 0.2	80 ± 5	199 ± 3

^aReference 7.

shown in Fig. 2(b). The peak values of the carrier density near zero time delay indicate that during the pump pulse, photoexcited carriers of $\sim 1.0 \times 10^{19} \text{ cm}^{-3}$ is generated for InN film, which is higher than its unintentionally doped carrier concentration [$(2.5 \pm 0.2) \times 10^{18} \text{ cm}^{-3}$]. On the contrary, pump pulse generates $\sim 2.3 \times 10^{19} \text{ cm}^{-3}$ of photoexcited carrier density for nanorods, which is of the same order to or lower than its free electron concentration.

Observed biexponential relaxation of InN film agrees with other experimental results, in which the carrier dynamics is found to be due to the hot carrier cooling through phonon emission followed by the defect-related nonradiative recombination process.^{1,2,5} The fast relaxation time of 30 ps measured for our InN film is consistent with that of 48 ps for InN film ($N_e = 1.2 \times 10^{19} \text{ cm}^{-3}$) measured by the optical pump-probe technique.¹ Meanwhile, previously measured near-infrared photoluminescence (PL) response shows that PL efficiency for nanorods is two orders of magnitude lower than that for InN epilayer,¹² indicating that nanorods have considerable amount of structural defects. Then the localized electrons within nanorods experience a preferential backward scattering caused by the increased structural defects¹² or a Coulombic restoring force from charged defects.¹³ The carrier scattering (or damping) time τ_0 related to the carrier conduction mobility through the Drude model is indeed shorter (13 fs) for nanorods than that for film (52 fs).⁷ The observed shorter scattering time of nanorods suggests a faster capture rate to the defect states, which further supports the existence of the high defect concentration of nanorods. Therefore, observed shorter initial relaxation time constant of nanorods compared to film can be explained by the inverse relation between the carrier lifetime and the free electron density due to the increased electron trapping by the defects.

It is well known that nonradiative defect-related recombination has the carrier-density-independent lifetime. To identify the nature of the recombination in InN nanorods, differential transmission is measured for the pump fluence range of 0.32–0.96 mJ/cm² (see Fig. 3). The general behavior of transmission trace for each sample is the same and the average fast relaxation time constant of nanorods is 2.1 ± 0.3 ps. The slow relaxation components for both samples also do not show any observable pump fluence dependence. The pump-fluence-independent carrier lifetime suggests that the defect-related nonradiative recombination rather than Auger recombination is the common recombination process for nanorods and InN film. At high pump fluence ($>0.6 \text{ mJ/cm}^2$), the maximum negative change in transmission $\Delta T_{\text{terahertz}}^{\text{max}}$ of InN film in Fig. 3(b) shows saturation, while that of nanorods scales linearly with the pump

fluence. The saturation of $\Delta T_{\text{terahertz}}^{\text{max}}$ for InN film can be described as trap saturation due to the high photoexcited carrier density exceeding free electron concentration. However, the photoexcited carrier density of nanorods at pump fluence below 1 mJ/cm² is still smaller than the free electron density so that photoexcited carrier density and subsequently $\Delta T_{\text{terahertz}}^{\text{max}}$ increase linearly with pump fluence.

Here we need to pay attention to the extremely slow relaxation time constant τ_2 observed for nanorods. In addition to the significant amount of defects, the physical properties of InN nanorods strongly depend on the geometrical nature of nanorods, such as high surface-to-volume ratio. Therefore carrier dynamics of nanorods can be sensitive to the carrier relaxation near the surface, which is significantly different from that of the bulk. In particular, it is known that the carrier diffusion reduces diffusion rate significantly near the surface.¹⁴ Since the lattice heating takes place on the extent region in which the energy transfer occurs by diffusion, reduced diffusion rate near the surface corresponds to the reduced heated volume. We assume that the effective diffusion distance has the form of a conventional diffusion length $(Dt)^{1/2}$ where t is the time for a hot carrier to diffuse before losing its energy by phonon emission.¹⁴ With the ambipolar diffusion coefficient of 2.0 cm²/s near the InN

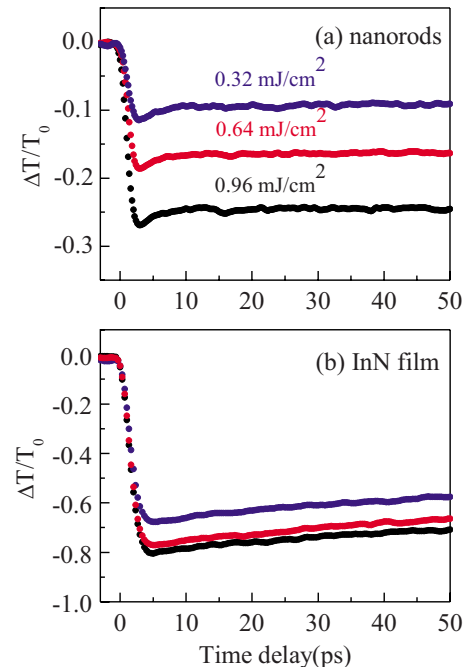


FIG. 3. (Color online) Pump fluence dependence of differential terahertz transmission for (a) InN nanorods and (b) InN film excited at the pump fluences of 0.32 (blue), 0.64 (red), and 0.96 mJ/cm² (black).

surface,² the corresponding diffusion length is about 45 nm in 10 ps, during which the lattice heating is achieved. This diffusion length is of the same order of the radius (average radius=65 nm) of nanorods, indicating that carriers within nearly the whole volume of nanorods participate in the carrier relaxation process. The carrier lifetime near the InN surface is particularly slow and is known² to be 5.4 ns. This value agrees well with our abnormally long relaxation time constant (≥ 7 ns) of nanorods, confirming that the carrier dynamics of InN nanorods is mainly governed by the carrier diffusion near the surface. Meanwhile, the same long relaxation of transient transmission response was observed for another InN nanorod sample⁶ with much higher aerial density ($8 \times 10^9 \text{ cm}^{-2}$) of rods (not shown here). For this sample, the aerial density is so high that the gaps between the rods are very small and thus the excitation light cannot propagate through the gaps to excite the carriers in Si substrate. Therefore, the nanosecond-order relaxation observed for both nanorod films is the intrinsic property of the nanorod layer, not due to the slow relaxation of photoexcited carriers in Si substrate.

IV. SUMMARY

We have investigated the carrier relaxation dynamics in InN film and InN nanorods using optical pump–terahertz probe spectroscopy. Biexponential relaxation fit to the differential transmission traces shows that the carrier dynamics of InN film and nanorods is due to the fast hot carrier cooling through phonon emission and the defect-related nonradiative recombination process. The pump-fluence-independent relaxation dynamics rules out nonlinear recombination process such as Auger recombination. The extremely long relaxation

time constant observed for nanorods indicates that the carrier relaxation process is dominated by the slow carrier diffusion in the vicinity of the surface, which is due to the geometrical characteristics of nanorods.

ACKNOWLEDGMENTS

The authors are grateful to Professor S. Gwo for the InN samples and helpful discussions and H.-Y. Chen for providing optical reflectivity data. This work was supported by the National Science Council (NSC) through NSC Grant No. 96-2112-M-009-016-MY3.

¹F. Chen, A. N. Cartwright, H. Lu, and W. J. Schaff, *J. Cryst. Growth* **269**, 10 (2004).

²F. Chen, A. N. Cartwright, H. Lu, and W. J. Schaff, *Appl. Phys. Lett.* **87**, 212104 (2005).

³Y.-C. Wen, C.-Y. Chen, C.-H. Shen, S. Gwo, and C.-K. Sun, *Appl. Phys. Lett.* **89**, 232114 (2006).

⁴T.-R. Tsai, C.-F. Chang, and S. Gwo, *Appl. Phys. Lett.* **90**, 252111 (2007).

⁵V. Pačebutas, G. Alecksejenko, A. Krotkus, J. W. Ager III, W. Walukiewicz, H. Lu, and W. J. Schaff, *Appl. Phys. Lett.* **88**, 191109 (2006).

⁶H. Ahn, Y.-P. Ku, Y.-C. Wang, C.-H. Chuang, S. Gwo, and C.-L. Pan, *Appl. Phys. Lett.* **91**, 132108 (2007).

⁷H. Ahn, Y.-P. Ku, Y.-C. Wang, C.-H. Chuang, S. Gwo, and C.-L. Pan, *Appl. Phys. Lett.* **91**, 163105 (2007).

⁸S. Gwo, C.-L. Wu, C.-H. Shen, W.-H. Chang, T. M. Hsu, J.-S. Wang, and J.-T. Hsu, *Appl. Phys. Lett.* **84**, 3765 (2004).

⁹K. P. H. Lui and F. A. Hegmann, *J. Appl. Phys.* **93**, 9012 (2003).

¹⁰M. van Exter and D. Grischkowsky, *Phys. Rev. B* **41**, 12140 (1990).

¹¹H. Ahn, C.-H. Shen, C.-L. Wu, and S. Gwo, *Appl. Phys. Lett.* **86**, 201905 (2005).

¹²C.-H. Shen, H.-Y. Chen, H.-W. Lin, S. Gwo, A. A. Klochikhin, and V. Yu. Davydov, *Appl. Phys. Lett.* **88**, 253104 (2006).

¹³J. B. Baxter and C. A. Schmuttenmaer, *J. Phys. Chem. B* **110**, 25229 (2006).

¹⁴E. J. Yoffa, *Appl. Phys. Lett.* **36**, 37 (1980).